



Chart-Based Granular Slope Stability Assessment Using the Modified Mohr–Coulomb Criterion

Jian Zhou¹ · Chuanqi Li¹ · Panagiotis G. Asteris² · Xiuzhi Shi¹ · Danial Jahed Armaghani³

Received: 28 July 2021 / Accepted: 9 November 2022 / Published online: 30 November 2022
© The Author(s) 2022

Abstract

There are usually two types of slopes in nature: soil and rock. However, the granular slope has gradually come into view and has caused concern. In this paper, a modified Mohr–Coulomb (MC) criterion has been proposed to estimate the strength parameters of medium materials using a new parameter (τ_0) instead of the traditional MC parameter (c). Meanwhile, there is a new stability chart of a granular slope whose core is the dimensionless stability number N_s and dimensionless coefficient DR based on a modified MC criterion to estimate the safety factor of a granular slope preliminarily when the geometric and strength parameters of the slope are determined. A practical case is introduced to test the results, showing that the stability chart proposed in this paper is applicable to granular slopes. The research content and the proposed new viewpoints are intended to offer preliminary judgments on the stability analysis of granular slopes and provide guidance for the stability analysis and construction design of granular slope engineering.

Keywords Granular slope · Modified Mohr–Coulomb criterion · Slope stability · Stability chart · Dimensionless stability number and coefficient

1 Introduction

Slopes are common engineering geological bodies in nature. With the gradual acceleration in the pace of human exploration of nature, an increasing number of projects are developed with slopes as the objects of development, such

as tunnels, railways and dams [1–7]. However, in engineering practice, debris flow, landslide, collapse and rock-fall are common disasters caused by slope instability caused by external factors [8–11]. Therefore, slope stability has always been one of the key issues in geotechnical engineering. To ensure the safe and efficient development and protection of slopes, different analysis methods have been developed to simply and efficiently determine the existing slopes stability, including deterministic analysis [12–14], numerical simulation [15–17], statistical analysis [18–20] and artificial intelligence techniques [21–32].

Among the many methods of slope stability analysis, the chart method was established early and applied to analyze common slope (soil slopes and rock slopes) works in nature. Taylor [33] first proposed a chart to calculate the safety coefficient of a simple homogeneous slope; however, the calculation of the safety coefficient needs to go through a complex iterative process. To abandon complex iterative operations, Michalowski [34] proposed a kinematics method based on the limit analysis method to establish a new type of slope stability calculation chart. Klar et al. [35] made a new chart explanation for the calculation of the safety factor (SF) of soil slopes. Sun and Zhao [36] introduced a set of stability charts for homogeneous soil slopes based on Klar's research

✉ Panagiotis G. Asteris
panagiotisasteris@gmail.com

✉ Danial Jahed Armaghani
danialarmaghani@susu.ru

Jian Zhou
csujzhou@hotmail.com

Chuanqi Li
lcqchuanqicsu@gmail.com

Xiuzhi Shi
baopo@csu.edu.cn

¹ School of Resources and Safety Engineering, Central South University, Changsha 410083, China

² Computational Mechanics Laboratory, School of Pedagogical and Technological Education, 14121 Heraklion, Athens, Greece

³ Department of Urban Planning, Engineering Networks and Systems, Institute of Architecture and Construction, South Ural State University, Chelyabinsk, Russia



work and considered the effects of pore water pressure as one of the influential factors on slope stability. Eid [37] designed a graph for the stability of cohesive soil homogeneous slopes and added a chart to determine the sliding SF under static and dynamic loads. Vo and Russell [38] provided an illustration of slope stability for solving the problem of a heterogeneous unsaturated soil slope. At the same time, there are also a few scholars who have utilized the chart method to study and contribute to the stability of rock slopes. Carranza-Torres [39] first proposed a chart to analyze the stability of rock slopes with the Hoke Brown (HB) parameter, $a = 0.5$ and a single slope angle. Li et al. [40] proposed a graph based on the parameters in the HB criterion to evaluate rock slope stability and systematically plotted the stability results under different disturbances and earthquakes [41, 42]. Shen et al. [43] recommended a new stability graph based on HB parameters to estimate the SF values using the limit equilibrium method and developed a new way to calculate the SF considering the disturbance factor and the slope angle. Sun et al. [44] used the strength reduction technique to map the stability of rock slopes under specific angles and disturbance factors. In this way, they estimated the safety coefficient of slopes simpler and faster by using HB failure criterion parameters directly.

In previous studies, the stability analysis of the soil slope was based on the Mohr–Coulomb (MC) failure criterion, and the rock mass of the rock slope meets the HB criterion due to its nonlinear strength, as shown in Fig. 1. However, there is a kind of engineering body called a granular slope (GS) that is formed by accumulating medium material (e.g., waste rock, metal, ore, gypsum and gangue). So, from the macro-point of view, a GS does not belong to the soil slope, nor does it belong to the seemingly complete rock slope. Therefore, both the traditional MC criterion and the generalized HB criterion could be inadequate to accurately describe the strength properties of a GS with medium material.

Based on medium mechanics, this paper proposes a modified MC criterion to calculate the SF of a granular slope. Then, combined with the characteristics of medium parameters, a granular slope stability chart is provided to simple and fast through preliminary and repose of SF chart for subsequent repose of slope stability analysis and provides certain guidance for management.

2 Modified MC Method

2.1 Transnational MC Criterion

Using a series of test results on sandy soil, Coulomb [45] concluded that the shear strength of soil is in the stress range with some small changes, which could be expressed as a

linear function of normal stress on the shear sliding surface:

$$\tau = \sigma \tan \varphi \quad (1)$$

where φ is the internal friction angle of the soil, $\tan \varphi$ is called the coefficient of the internal friction of soil, τ is the ultimate shear stress on the shear sliding surface, and σ is the stress on the vertical shear sliding surface.

Subsequently, Coulomb [45] proposed a general shear strength formula based on the test results of cohesive soil as follows:

$$\tau = c + \sigma \tan \varphi \quad (2)$$

where c is undrained cohesion values.

Mohr [46] mentioned that when the shear stress on a section of a material reaches a certain value related to normal stress on the surface, the material undergoes shear failure. This function is a curve in a Cartesian coordinate system that is commonly referred to as the Mohr envelope, as shown in Fig. 2 (a). Many scholars have processed the Mohr envelope according to the strength test data in different mathematical forms. The parabolic, hyperbolic, cycloid, straight line and other forms of approximation of the real experience curve have appeared. However, most of the related researchers agreed that in a case where the stress on the material is not a large amount, the linear MC strength curve (Fig. 2 (b)) tends to yield better results.

According to the traditional MC criterion, in the destruction of soil and rock masses, the cohesive force (cohesion, c) and φ are the strength parameters of the material. In other words, c and φ are attributes of the material itself. According to the explanation of c in the dictionary, the attraction between adjacent parts within the same substance is a manifestation of molecular force. It can be judged from the above knowledge that the true c is a microforce, which may exist in the macroscopic pure soil and rock mass material with complete individuals. Therefore, it is persuasive to use the MC criterion to consider c as a fixed value in such material.

As shown in Fig. 3, it is found from the triaxial shear test that greater φ values lead to greater compressive strength and shear resistance. In addition, greater c values lead to a larger difference between the maximum and minimum principal stresses. Wang [47] introduced an equation for estimating the rock's cohesion under different stress states according to different. Since a crack inside a rock cannot be observed, φ values obtained from the end of the strength test are normally used in studies related to rock mechanics. At the same time, it is noted that the cohesive force is not a kind of force but represents the ability of the rock to bear various forces, which is controlled by the initial force and is not a fixed value.

Compared with the internal structure of rock and soil material, the “independence” of granular materials is more

Fig. 1 Relationship between HB and equivalent MC envelopes

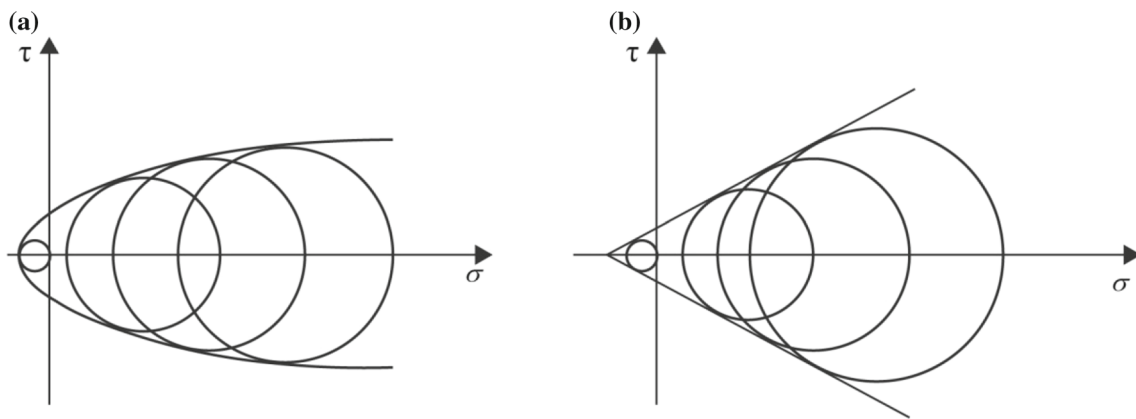
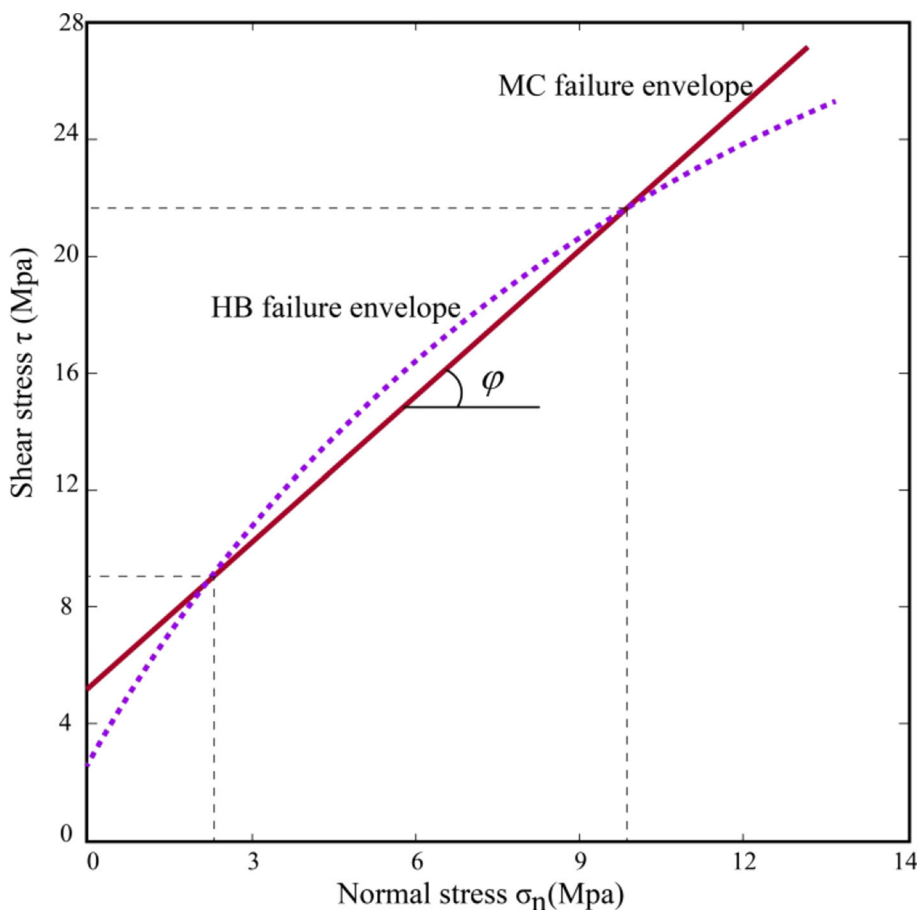


Fig. 2 Mohr envelope and MC strength curve

obvious at the macrolevel, as shown in Fig. 4. Granular materials contain discrete elements of different sizes, which prove that there is no cohesive force generated by intermolecular forces at the macrolevel.

As displayed in Fig. 5, there is no cohesive force or c in the ideal medium material. In fact, the interaction between the medium materials is completely balanced by the friction force. Failure means that the shear stress on a certain section exceeds the combined force of the internal friction force and

the bite force between the element materials. For general medium materials, it is very important to find the true c values to be used in the MC criterion.

2.2 Limit Equilibrium of Granular Materials

Wang [47] introduced an equation for solving the rock cohesion in different states according to different variations in rock cohesive forces:

Fig. 3 MC strength curve (resulting from triaxial shear test)

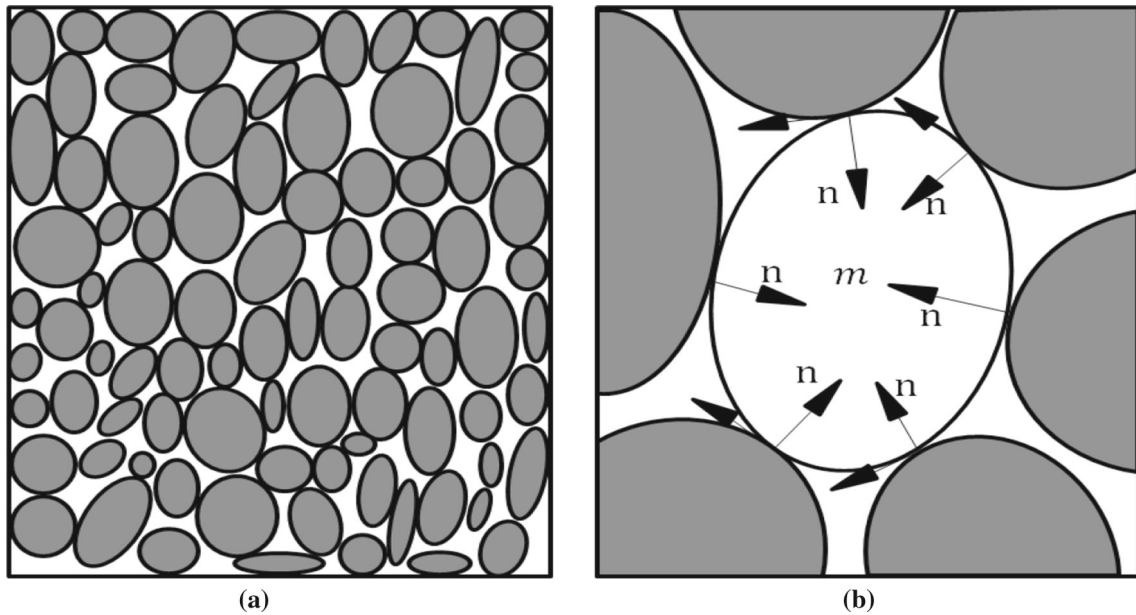
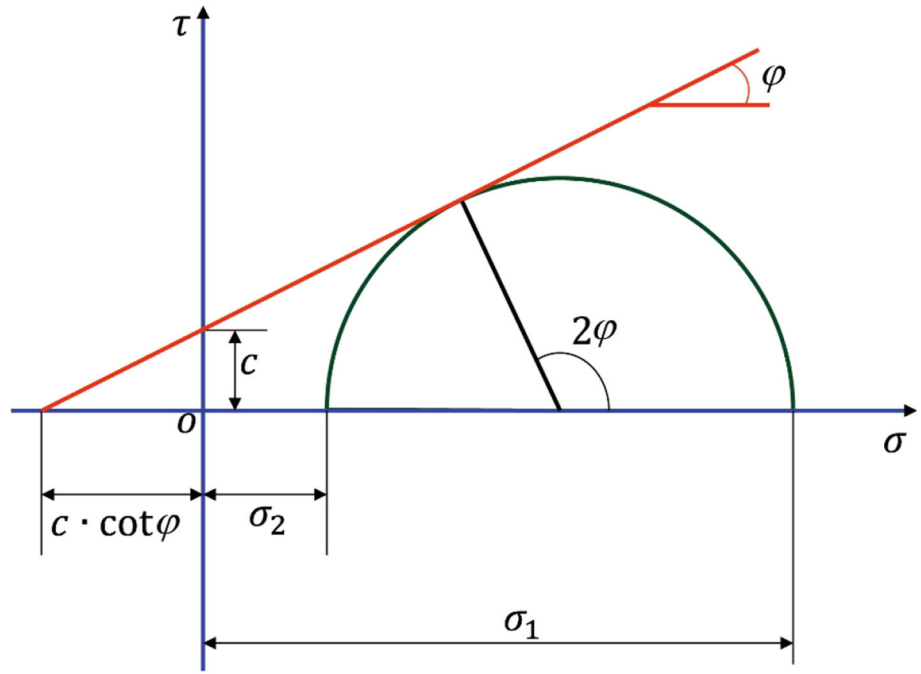


Fig. 4 Force on medium particles, **a** medium particle distribution and **b** particle forces

Uniaxial pressure state:

$$c = \frac{1}{2} \sigma_1 \tan \alpha \tag{3}$$

$$c = \sigma_1 \frac{1 - \sin \varphi}{2 \cos \varphi} \tag{4}$$

where σ_1 is the vertical main pressure of the rock mass, is the external collapse angle, and φ is the internal friction angle of the rock. When $\varphi=0$ and $\alpha=45^\circ$, c will be the maximum amount.

Two-axis unequal pressure state:

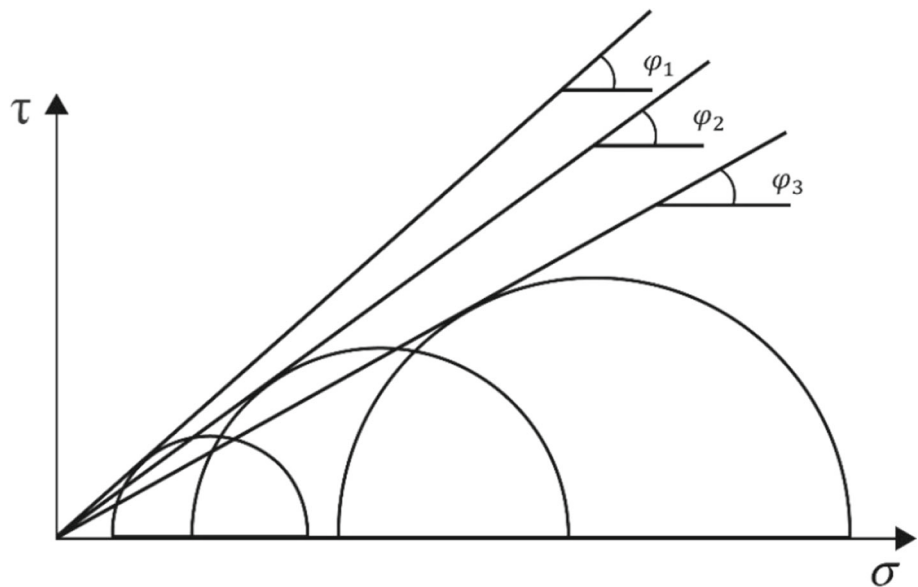
$$c = \frac{(1 - \sin \varphi) \sigma_1 - (1 + \sin \varphi) \sigma_2}{2 \cos \varphi} \tag{5}$$

where σ_1 and σ_2 are the maximum and minimum principal stresses applied to the rock specimen, respectively.

Triaxial unequal pressure state:

$$c = \left(\frac{R_0}{r} \right) \sigma_0 \frac{\tan \alpha}{3} \tag{6}$$

Fig. 5 Curve of ultimate shear stress of non-cohesive medium materials



$$c = \left(\frac{R_0}{r}\right) \sigma_0 \frac{1 - \sin \varphi}{3 \cos \varphi} \tag{7}$$

where σ_0 is the maximum principal tangential stress in the surrounding rock.

In this paper, a limit equilibrium experiment is adopted to explore the strength parameters of the MC criterion for general viscous medium materials (Fig. 6), material density γ of viscous medium materials, local gravity acceleration, g , and packing height, h_0 . The vertical pressure at point o is equal to $\gamma h_0 g$ in Fig. 6, and it cannot act on point o in the horizontal direction, which is equivalent to the maximum and minimum principal stress. Therefore, the stress state at point o is represented in Fig. 6.

In Fig. 6, the longitudinal intercept, τ_0 , represents the initial shear stress of general medium materials during initial accumulation. By geometric drawing, the known stress circle radius and φ can be used to solve τ_0 :

$$\tau_0 = \frac{h_0 \gamma g}{2} \frac{\cos \varphi}{1 + \sin \varphi} \tag{8}$$

According to the above equation, it is shown that the initial shear stress of the medium material in the experiment is related to the initial vertical stress and the internal friction angle carried by the medium material in general viscous accumulation, which directly verifies that the cohesive force is not a fixed value Wang [47]. The medium material of the initial stress is not affected by the macrodiscreteness of the repose on the material, regardless of the form and function, and the inner cohesion of the soil and rock mass is roughly the same.

In this paper, the stability of the granular slope is not studied by the cohesion force, which is one of the strength

parameters of the traditional MC criterion, but by the initial shear stress τ_0 of the medium material proposed in this paper, which is controlled by the height of the piled medium material and its internal friction angle.

2.3 Modified MC Criterion

The limit equilibrium formula of the general viscous medium material is shown as follows:

$$\tau = \tau_0 + \sigma \tan \varphi \tag{9}$$

According to previous studies, this paper proposes a suitable shear strength formula for medium material based on the modified MC criterion.

$$\tau = \frac{\gamma_t g h_0}{2} \cdot \frac{\cos \varphi}{1 + \sin \varphi} + \sigma \tan \varphi \tag{10}$$

where γ_t is the medium material density during the test, h_0 is the maximum height (40 cm) of the standard direct shear apparatus, φ is the internal friction angle of the medium material, σ is the normal stress and τ is the shear stress.

In the traditional MC failure criterion, c and φ are determined from the shear strength experiment. In the modified MC criterion, the initial shear stress, which is similar to c , is related to γ , material stacking height, density and other parameters. It shows that γ can still be obtained from the conventional shear strength test, and the initial shear stress can be calculated according to the test results. It can be found from the actual test results (Fig. 7) that when the traditional MC parameters obtained from the medium material are used to analyze the actual engineering body, results with large deviation are often achieved (ultrahigh safety factor).

Fig. 6 **a** Curve of the ultimate shear stress of viscous medium materials and **b** accumulation of viscous medium materials

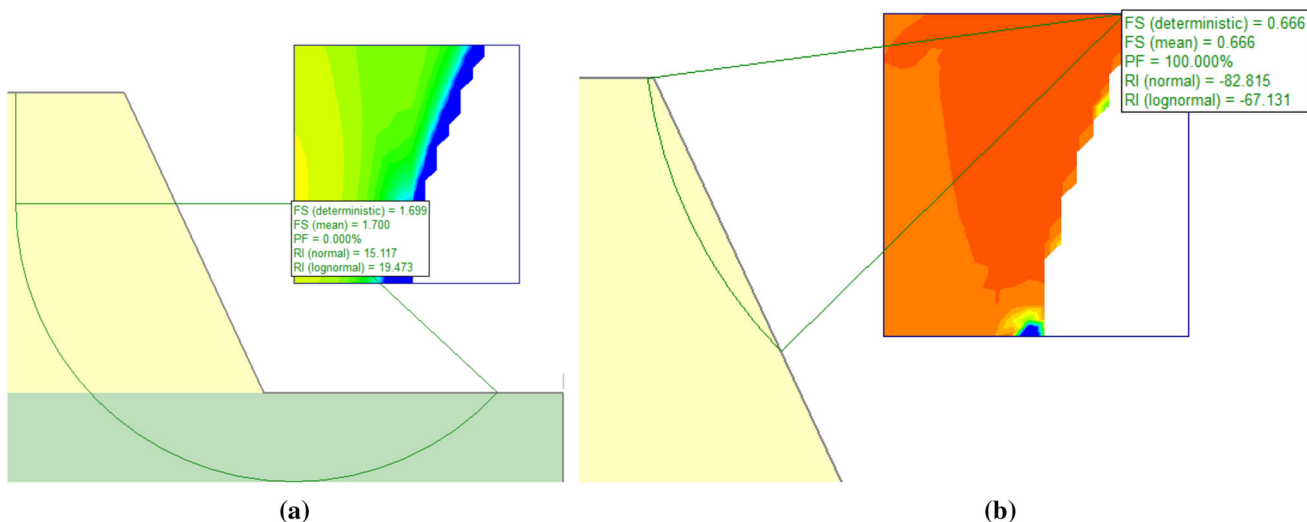
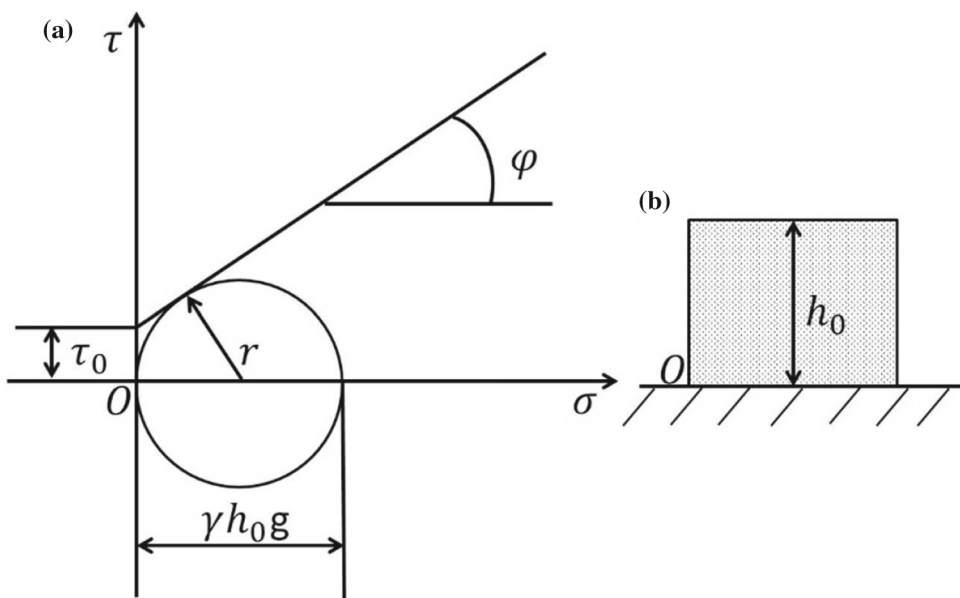


Fig. 7 Stability of a granular slope with traditional MC and modified MC strength parameters, **a** cohesive force from test and **b** initial shear stress

As shown in Fig. 7, when c obtained from the direct shear strength test is an input of the software, the SF of the granular slope will obviously exceed the standard safety value (the instability probability is definitely zero). By comparison, when the parameters in the modified MC criterion are software inputs, the SF of the slope with loose mass is significantly reduced (instability probability is high). It is obvious from the field observation in Fig. 8 that when c values obtained from the test are input, the judgment of the stability of the granular slope is seriously distorted. On the other hand, the c value obtained from the modified MC formula after participating in the analysis shows only a small difference from the actual situation.

3 Stability Number Based on the Modified Mohr–Coulomb Criterion

3.1 Traditional MC Stability Number for Soil Slope

Taylor [33] suggested the use of the dimensionless variable stability number to analyze the stability of the soil slope (Fig. 9), which can be defined as:

$$N = \frac{c_d}{\gamma H} = \frac{c}{\gamma HSF} \tag{11}$$

where γ is the unit weight of a single soil layer, H is the vertical height of the slope, SF is the safety factor, and c is soil cohesion.

Fig. 8 Actual situation of a granular slope

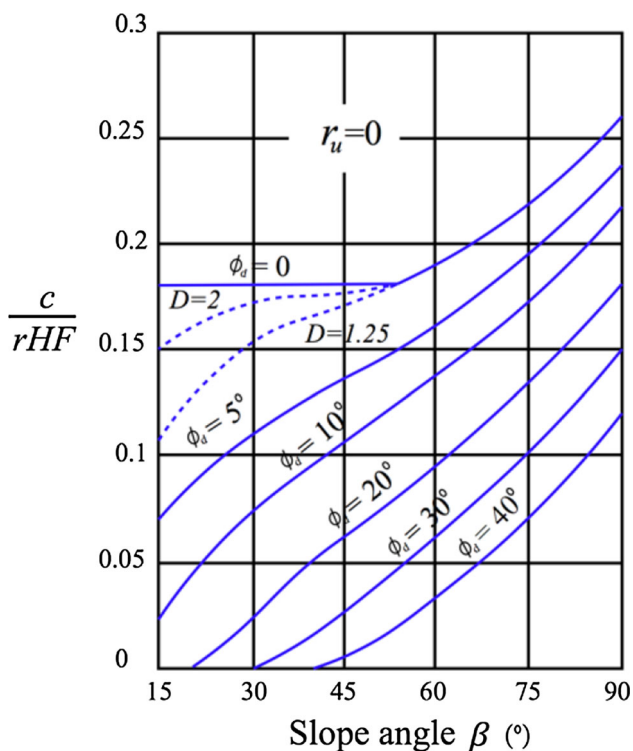


Fig. 9 Stability number of uniform slopes [17]

Bell [48] proposed a modified dimensionless number, N^* to make the dimensionless number of the stability number independent of the SF.

$$N^* = \frac{c_d}{\gamma H \tan \phi_d} = \frac{c/SF}{\gamma H (\tan \phi/SF)} = \frac{c}{\gamma H \tan \phi} \quad (12)$$

However, the calculation of the safety coefficient of the cohesive-frictional soils slope through Taylor’s stability chart requires complex iteration. Steward et al. [49] proposed a stability chart without iterative calculation for the estimation of the safety coefficient of the cohesive-frictional soils slope, as shown in Fig. 10.

Based on Steward et al.’s chart, the abscissa is c/HF , and the ordinate is $\tan^2 \beta / F$. When solving F , $c/H \tan^2 \beta$ should be determined first, then input the slope angle, find the unique coordinate point (x, y) in the figure and finally establish the equation to solve the coordinate value and the horizontal and vertical coordinate expression and verify whether the F value is reasonable in the allowable range of error.

3.2 HB Stability Number for Rock Slopes

Similarly, in the rock slope stability chart, the dimensionless stability number is defined as:

$$N = \frac{\sigma_{ci}}{\gamma H SF} \quad (13)$$

where SF is the slope safety factor, γ is the unit weight of the rock mass, H is the slope height, and σ_{ci} is the uniaxial compressive strength (UCS) of the rock mass [40].

Shen et al. [43] studied the concept of the strength rate used in tunnel research and correlated it with the stability number [50]. When the HB parameters (i.e., GSI, mb, s and a) are determined, the SF of the rock slope is only related to the strength rate. These parameters can be plotted as a series of graphs (Fig. 11) to characterize the relationship between

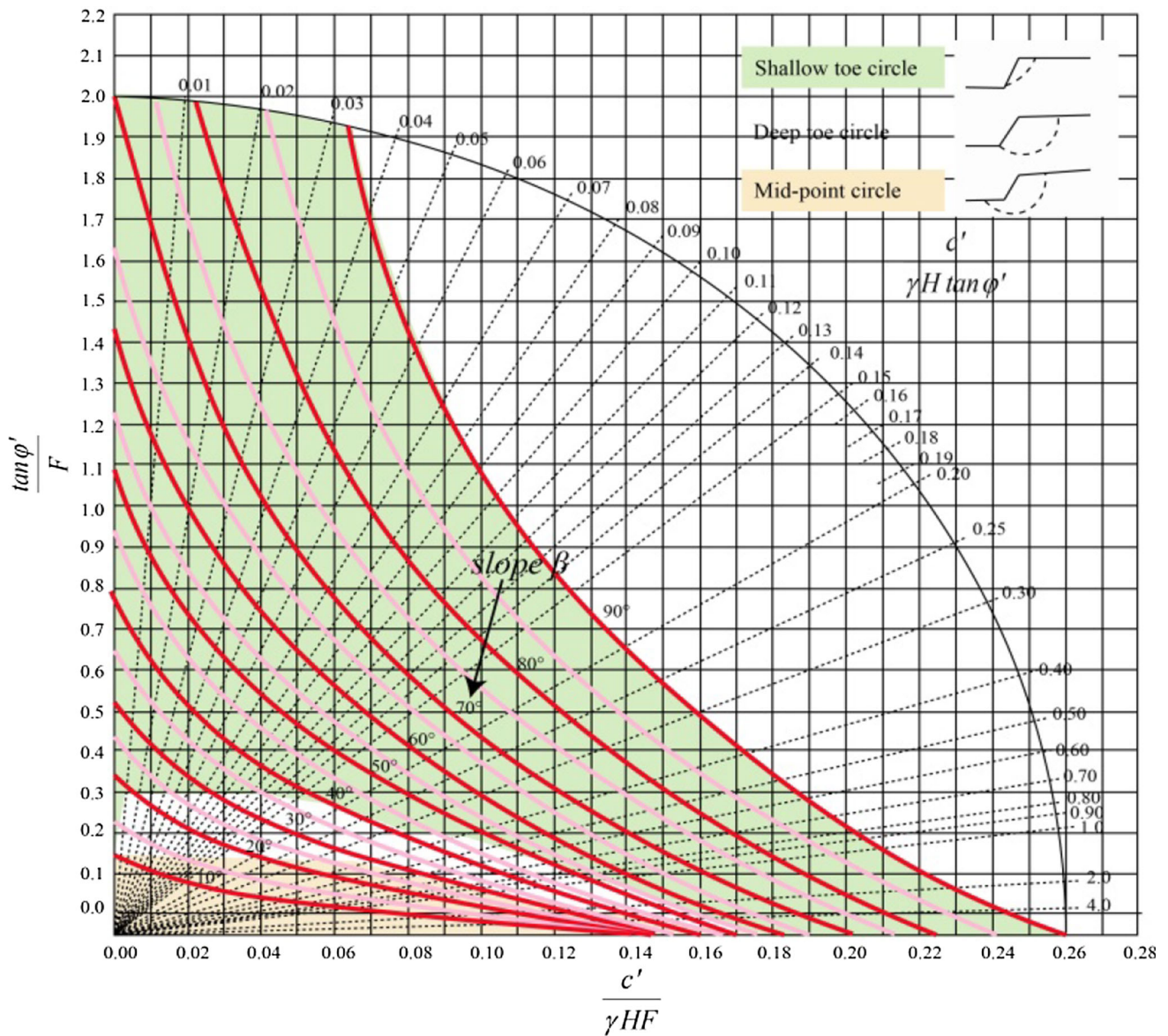


Fig. 10 Slope stability design chart for cohesive-frictional soils [49]

the SF and strength rate (SR) under different HB parameters [51].

Carranza-Torres [39] further studied the HB criterion and found that when the HB parameter $a = 0.5$, the rock slope SF is only related to three independent variables: \bar{H} , s/m_b^2 and β . The function that is combined with the three independent variables is modified as follows:

$$\bar{\gamma H} = \frac{\gamma H}{\sigma_{ci} m_b} + \frac{s}{m_b^2} \tag{14}$$

In Fig. 12, the abscissa is a combination of the three independent variables, and the ordinate is the slope SF. When the values of m_b and s are calculated using the generalized HB criterion proposed by Hoek et al. [51], except for the angle,

the remaining two independent variables can also be calculated. Finally, based on the known values, the SF values can be obtained directly in the chart.

3.3 Modified MC Stability number for Granular Slopes

By reviewing the application of the stability number in the stability charts of soil and rock slopes, a common point that the factors in the expression of the stability number are related to their respective media can be found. For example, the molecules of two kinds of stability numbers represent one of the characteristic properties of soil materials and rock

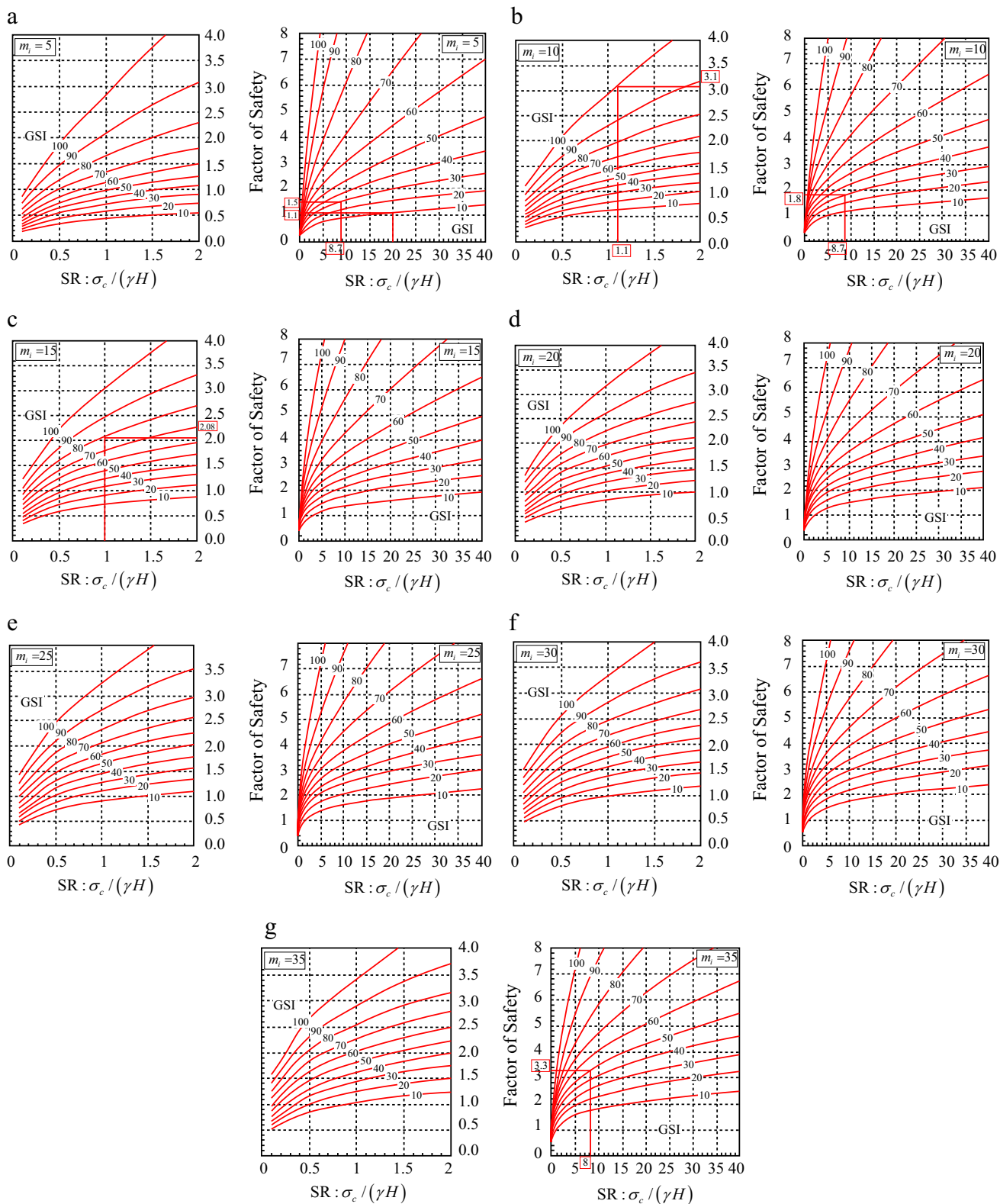
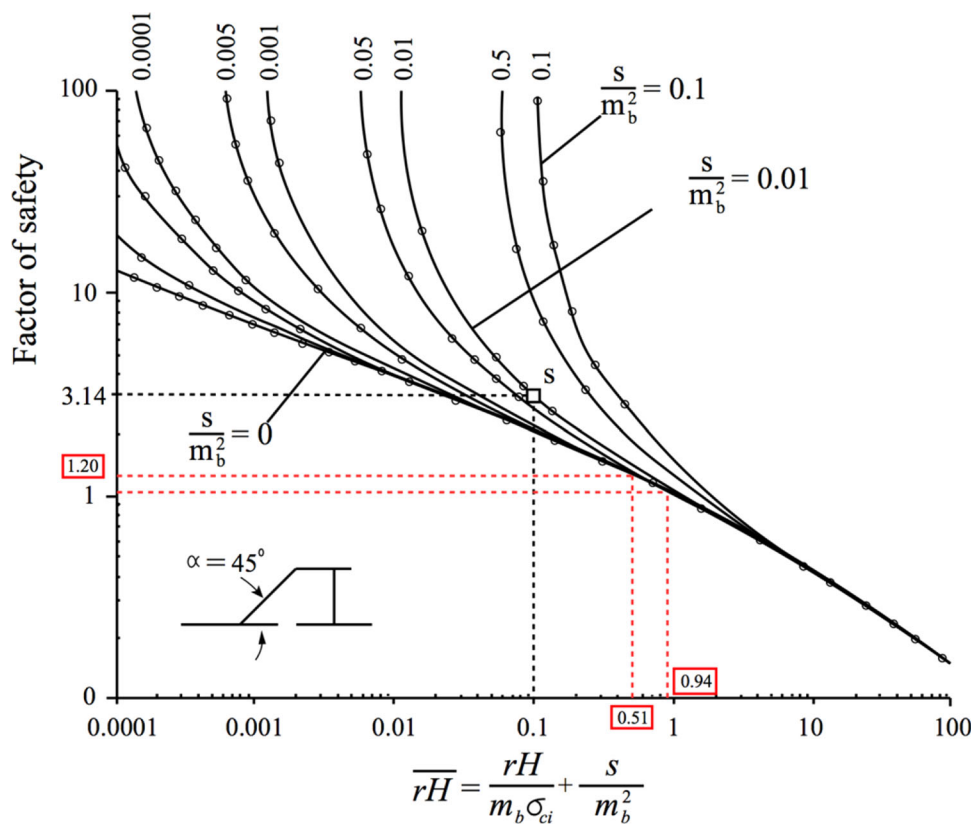


Fig. 11 Proposed stability charts for rock slope angle = 45 and D = 0 (5 < m_i < 35) [43]

Fig. 12 Slope stability chart ($\beta = 45^\circ$ $a = 0.5$) [39]



masses. Therefore, the two mentioned dimensionless stability numbers are not applicable to the chart analysis of the stability of granular slopes for two reasons:

A: From the macroscopic point of view, there is no intermolecular force between the medium materials in the granular slope, and the macroscopic equilibrium is basically maintained by a series of physical actions such as interparticle friction.

B: From the point of view of laboratory tests, the core sampling of the granular slope cannot be carried out, so the UCS test cannot be carried out σ_{ci} .

Based on Taylor [33] study, the following dimensionless stability number was applied to the granular slope in this paper.

$$N_s = \frac{\gamma HSF}{\tau_0} = \frac{\gamma HSF}{\frac{\gamma_l g h_0}{2} \cdot \frac{\cos \varphi}{1 + \sin \varphi}} \tag{15}$$

where γ_l is the weight of the medium material unit in the direct shear test, γ is the weight of the medium material unit in the granular slope, H is the granular slope height, SF is the safety factor of the granular slope, g is the local gravitational acceleration, h_0 is the maximum loading height of the shear instrument for medium materials, and φ is the internal friction angle obtained by the shear test.

In addition, during the stacking process, the density of medium materials in the granular slope will be different from that of the medium density in the test due to vibration and compaction, and the variation range of medium material is generally from 1.05 to 1.52 g/cm^3 [52]. At present, researchers often choose medium density as the experimental density in the actual direct shear test. Based on this, this paper proposes a dimensionless number DR , which is defined as the ratio of the field density of the granular slope to the experimental medium density so that the field density change is incorporated into the depiction of the stability chart to more accurately solve the stability of the granular slope.

4 Chart Method for Granular Slope Based on Modified MC

Taylor [33] identified three types of failure slip planes for soil slopes, i.e., toe circles, slope circles, and midpoint (or base) circles, as shown in Fig. 13. The appearance of different slip surface shapes is not only limited to slope height and the height from the top of the slope to the formation, but more importantly, it is related to the slope angle.

In this paper, two-dimensional software, i.e., Slide 6.0, which is popular in the field of geotechnical engineering, was used to analyze the granular slopes. After fitting thousands of

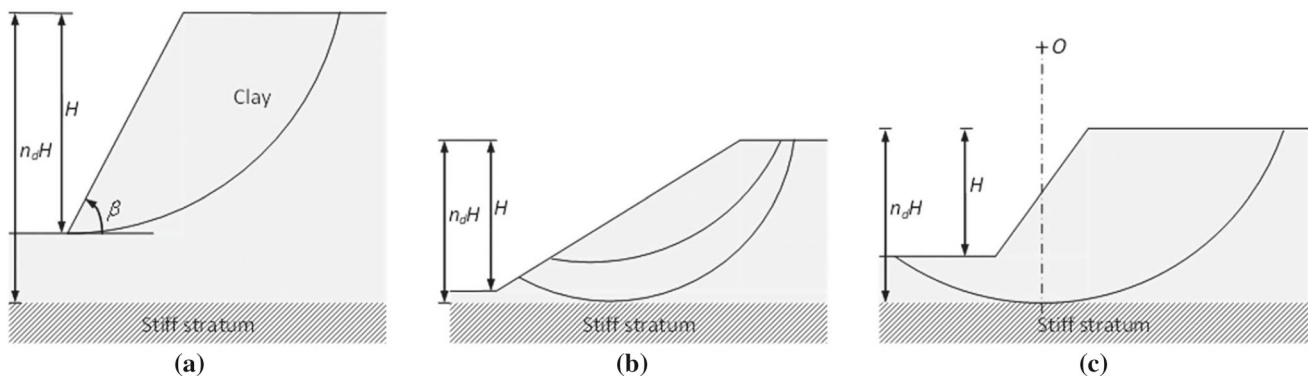


Fig. 13 Slip circles: **a** toe circle; **b** slope circle; and **c** midpoint circle [33]

test data, the relationship between the angle of the granular slope and the dimensionless number, N_s , under the different DR can be found as follows:

1. With the increase in the slope angle, the value of the stability number has been on a downward trend. The stability numbers for slope angles less than 30 degree are significantly higher than those for slope angles greater than 30 degree, indicating that the influence rate of slope angle on the safety coefficient in a granular slope is different. When the slope angle is less than 30 degree, small changes in the slope angle may also cause a large change in the slope safety coefficient. In contrast, when the slope angle is greater than 30 degree, even if the slope angle changes considerably, the slope safety coefficient will not significantly change.
2. II. This paper studies the relationship between β and stability number. According to Fig. 14, under the same slope angle, the stability number increases with the increase in β , which indirectly verifies that β cannot be 0 in the stability of a granular slope. This is quite different from the traditional MC criterion used in the strength parameter analysis of soil slopes (stability chart friction angle = 0 [33]), so the existence and value of β are crucial to the stability of granular slopes.
3. III. Based on the research conducted by Huang [52], a general variation range of medium material density was introduced as (1.05–1.52 g/cm³). A stability chart for granular slopes with different β and DR values is displayed in Fig. 14. According to this figure, the DR values are changed from 1 to 1.52 g/cm³, the maximum values of N_s are 159.5, 169.8, 235.3, and 275.0, and the maximum and minimum β values are considered 55 and 15 degrees.
4. IV. In this paper, we modified four slide circles—“surface,” “top + surface,” “top + bottom” and “bottom + surface,” which occur in granular slopes, as shown in Fig. 15. It can be clearly observed that the main slide

circles are “surface” and “top + surface” when DR = 1. With the increase in DR values, the main slide circle also changed, and the ratio of “top + bottom” and “bottom + surface” gradually increased. This indicates that there is a close relationship between DR and the stability of granular slopes. Meanwhile, considering safety factor responses of different slide circles under different DR values, the results show that a higher safety factor always occurs in slide circles of “top + bottom” and “bottom + surface.”

In this paper, the stability chart (which can be used for SF calculation) is put forward emphatically as shown in Fig. 16. It provides a direct, simple and efficient solution method for the initial design of a granular slope. The stability chart of a granular slope proposed in this paper takes the stability number as the abscissa and the tangent value of β as the ordinate and the ratio of the SF of the granular slope. The input parameters are β data obtained from the shear strength test and slope parameters (slope angle and slope height) of medium materials, so the unique data intersection point (x, y) can be directly found in the chart. Finally, the outputs of SF_x and SF_y take the average value of the SF within the allowable error range as the reference opinion for preliminary stability analysis.

It can be found from the arbitrary stability chart drawn in this paper that when mechanical and geometric parameters of the granular slope other than the slope angle are fixed, then, τ_0 /HSF and $\tan\beta$ /SF increase with the increase in the slope angle, which means that the SF of the slope decreases. When all the geometric parameters related to a slope are determined, τ_0 /HSF and $\tan\beta$ /SF increase with a decrease in β , and the SF values increase. At the same time, the comparison of the stability chart (a, b, c and d) shows that when the mechanical and geometric parameters of the slope are determined, the τ_0 /HSF and $\tan\beta$ /SF values decrease with increasing DR. This indicates that the SF is closely related to changing DR, and the regional SF with larger DR may be higher. This phenomenon is verified in the actual granular

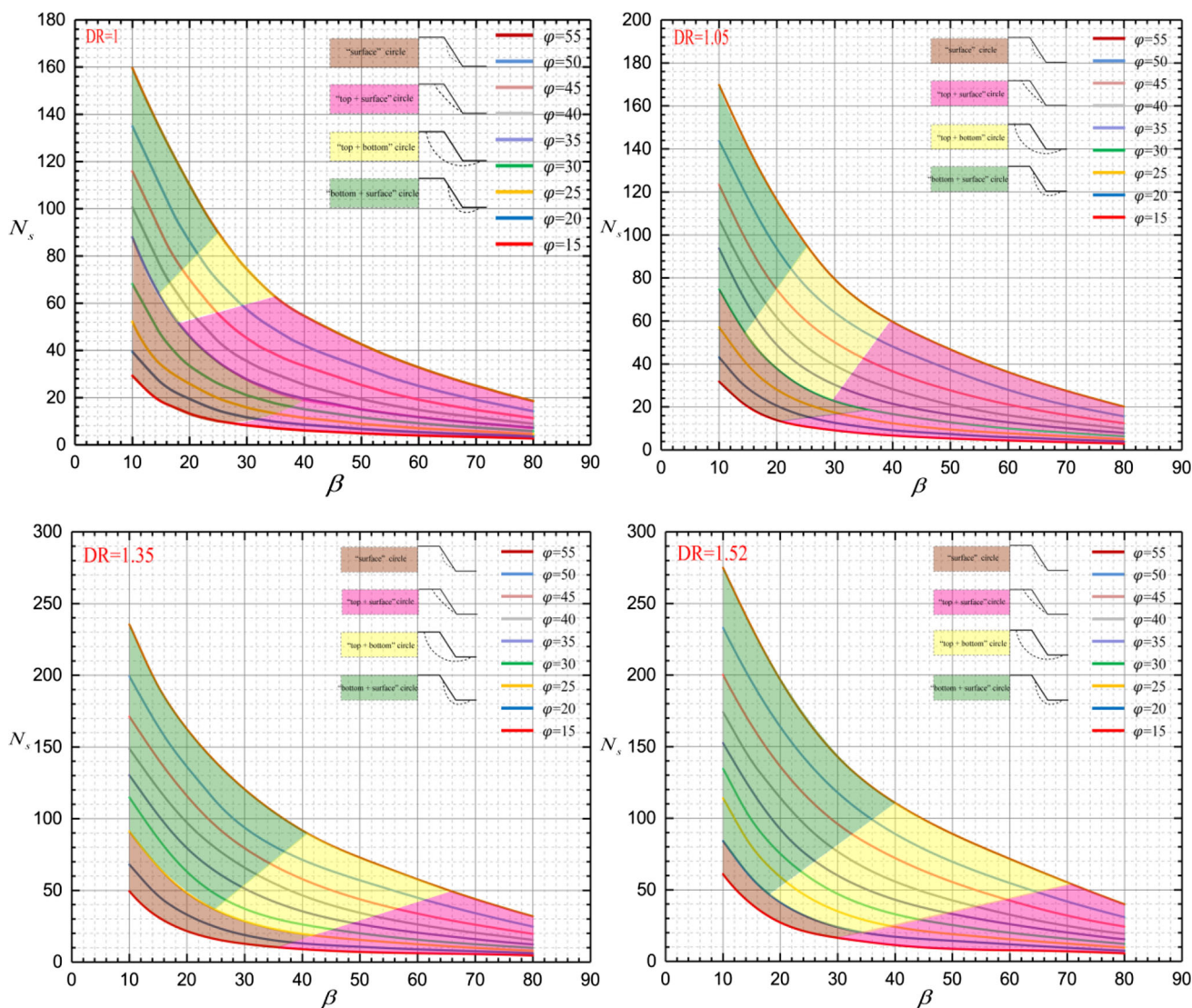


Fig. 14 Stability chart for granular slopes with different ϕ and DR values

slope, as shown in Fig. 16. From both field observations and experimental studies, it can be seen that the area with high slope density is concentrated in the central area at the top of the slope. The closer the area is to the slope surface, the smaller the density of the granular materials will be, until the density at the toe of the slope is almost the same as that of natural medium materials. At the same time, it can be seen from the field slope stability that the central region of the top of the slope body is in well-stability, the closer to the slope surface, the worse the regional stability is, and it is more likely to incur local collapse, edge crack and other adverse phenomena, which correspond to the meaning of the stability chart under the different DR proposed in this paper.

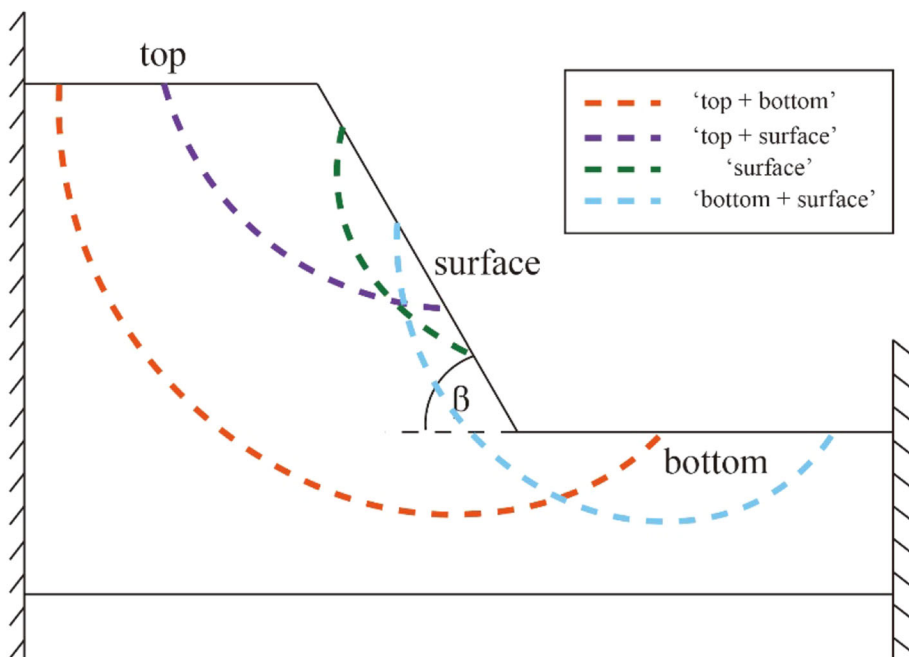
Figure 16 (a, b, c and d) contains more than 2000 sets of data. In contrast, Fig. 10 [49] shows that the stability diagram drawn of cohesive-frictional soils outside the dotted

line whose γ can approach 0 and 90 degrees, but the stability chart of granular slopes studied only considering the granular slope characteristics caused by the medium material itself whose internal friction angle is different from soil and rock materials in this article. Клейн [53] studied some physical properties of granular bodies and showed that γ in medium materials ranged from 15 to 55 degrees (see attached Table 1). And the internal friction angle of medium materials in stability chart for granular slope is considered range from 15 to 55 in this paper.

5 Case Study

This paper uses the modified MC criterion based on the chart method to evaluate the SF results of the waste rock slope

Fig. 15 Structure and slide circles of slopes



of the Fankou lead–zinc mine in Renhua County, Shaoguan City, Guangdong Province, China. In the following subsections, more details regarding this project will be given.

5.1 Site Investigation

The Fankou lead–zinc mine waste rock slope was built in the 1970s. It is mainly used for piling up the waste rock produced by excavation and blasting. After the waste rock is lifted from the underground to the surface, it is transported to the waste rock slope by car and discharged by bulldozer, with a daily discharge of approximately 300 ~ 400 tons. After a long period of mine production, a waste rock dump of approximately 20 m above the ground has been formed in the Fankou lead–zinc mine, as shown in Fig. 17. The waste rock pile site is located in the upper part of the original tailings pond. The average elevation at the bottom of the pile site is 108 ~ 109 m, and the average elevation at the top is 129 ~ 130 m. The whole pile is made up of the waste rock layer-by-layer from the underground hoisting. The north side of the waste heap site is close to the highway, and the slope angle ranges from 30 to 40 degrees. The overall slope surface is similar to a straight line and smooth. The angle of the south slope is between 40 and 50 degrees.

The Fankou lead–zinc mine granular slope, which is made of waste rock, is completely formed by the accumulation of hauled waste rock materials. This material is different from both the soil slope with high cohesion and the rock slope with good rock mass integrity. At present, there have been some regional collapses and landslides on the granular slope, so it

is very important to conduct effective stability evaluation on the granular slope.

5.2 Parameter Acquisition

Four specific locations (Fig. 18) were selected for the stability analysis of the granular slope (the slope height was fixed at 20 m), which was made of waste rock.

According to the modified MC criterion, first, it is necessary to perform physical and mechanical experiments on medium materials to obtain strength parameters of the internal friction angle to simulate.

At present, the direct shear test and triaxial shear test are the main strength tests for medium soil material. In the triaxial shear test, triaxial shear equipment with a high degree of automation was used to measure the strength and obtain the relevant parameters. However, according to the feedback of actual results, the data of the triaxial test are often inaccurate because of the interference of external conditions. Therefore, this study used the manual direct shear instrument to conduct the direct shear test of medium material, as shown in Fig. 19. The direct shear data were recorded and are shown in Table 2 and Fig. 20. The relevant-modified MC criterion, mainly parameters and slope geometry, is shown in Table 3.

5.3 Stability Analysis

The four different positions of the granular slope for chart analysis were selected as case studies of this research. According to these positions and the stability chart in this paper, the unique coordinate corresponding to each of these

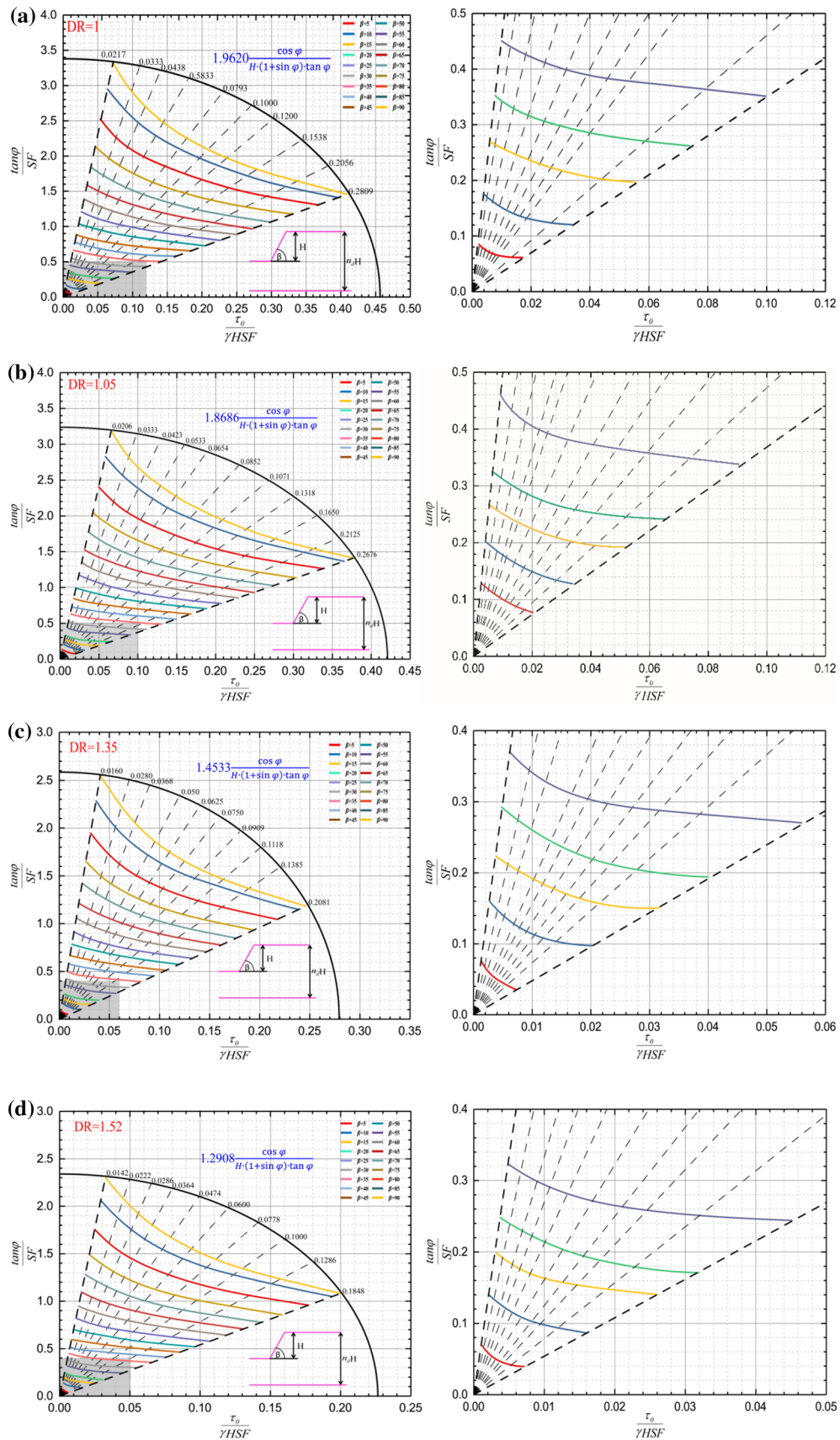


Fig. 16 Stability chart for granular slopes

Table 1 Internal friction angle of medium materials [53]

Medium materials	Density (t/m^3)	Internal friction angle (degree)	Unit cohesion force (kPa)
Iron ore	1.7 ~ 2	45	–
Soybean	0.6 ~ 0.8	32	–
Coarse gypsum	1.5	30	–
Fine gypsum	1.3	40	–
Saturated clay	1.9 ~ 2.2	15 ~ 25	1
Wet clay	1.7 ~ 1.9	25 ~ 35	20
Dry clay	1.6 ~ 1.7	40 ~ 45	200
Alumina	1.1 ~ 1.3	28 ~ 30	–
Pea	0.8	25 ~ 28	–
Saturated gravel	1.9 ~ 2.0	25 ~ 35	–
Dry gravel	1.8	35 ~ 45	–
Buckwheat	0.6 ~ 0.7	35	–
Saturated humus	1.7	28 ~ 30	1
Wet soil	1.6	30 ~ 45	5
Dry soil	1.2 ~ 1.5	28 ~ 35	50
Cultivated soil	0.85 ~ 1.3	30 ~ 36	–
Plant ash	0.4 ~ 0.7	40 ~ 50	–
Quick lime	0.8 ~ 1.1	30 ~ 45	–
Hydrated lime powder	0.6 ~ 0.7	30 ~ 45	–
Crushed limestone	1.4 ~ 1.7	35 ~ 55	–
Rock block	1.3 ~ 2.0	37	–
Calcium carbide	0.9	28	–
Slag	1.3 ~ 1.5	33	–
Coke	0.35 ~ 0.7	30 ~ 50	–
Hemp seed	0.5 ~ 0.6	30 ~ 38	–
Cryolite	0.85 ~ 1.0	30 ~ 37	–
Corn	0.7 ~ 0.75	28 ~ 40	–
Manna croup	0.68	30 ~ 35	–
Sunflower shell	0.3	50	–
Flax seed	0.65 ~ 0.75	25	–
Crushed chalk	1.4	39	–
Rye flour	0.4 ~ 0.55	35 ~ 50	–
Wheat flour	0.45 ~ 0.65	30 ~ 45	–
Selection of nepheline	1.1 ~ 1.3	31 ~ 40	–
Oat	0.4 ~ 0.5	28 ~ 35	–
Wood sawdust	0.15 ~ 0.3	30 ~ 55	–
Bran	0.18 ~ 0.45	55	–
Scum	1.9 ~ 2.1	30 ~ 35	–
Saturated sand	2.0	20 ~ 25	–
Wet sand	1.7 ~ 1.8	40	–
Dry sand	1.5 ~ 1.7	30 ~ 45	–

Table 1 (continued)

Medium materials	Density (t/m^3)	Internal friction angle (degree)	Unit cohesion force (kPa)
Sunflower	0.42	33 ~ 45	–
Maiden cane	0.65 ~ 0.85	22 ~ 25	–
Wheat	0.65 ~ 0.80	25 ~ 35	–
Pulverized coal	0.7	15	–
Rice	0.5 ~ 0.8	40	–
Rye	0.65 ~ 0.80	25 ~ 35	–
Copper ore	1.9	–	–
Sugar	0.7 ~ 0.9	50	–
Beet seeds	0.27 ~ 0.30	38	–
Saltpeter	0.8 ~ 1.1	40	–
Caustic soda	0.5 ~ 1.25	35 ~ 45	–
Wheat skin	0.32 ~ 0.56	22	–
Salt	0.7 ~ 1.3	30 ~ 50	–
Crushed volcanic ash	1.4	43 ~ 50	–
Saturated subclay	2.1	20 ~ 25	1
Wet subclay	1.9	15 ~ 20	10
Dry subclay	1.6	20 ~ 40	100
Ammonium sulfate	0.8 ~ 0.9	40	–
Peat	0.3 ~ 0.7	45 ~ 50	–
Non classified lump coal	0.95	27 ~ 32	–
Crushed coal	0.8	35	–
Lignite	0.6 ~ 0.65	30 ~ 45	–
Phosphate rock powder	1.3 ~ 1.8	40 ~ 45	–
Ammonium fluoride	0.8 ~ 0.9	33 ~ 40	–
Cement	1.0 ~ 1.6	27 ~ 40	–
Lentils	0.6 ~ 0.85	25 ~ 35	–
Slag	0.6 ~ 1.0	30 ~ 50	–
Crushed rock	1.3 ~ 2.0	40 ~ 45	–
Carbon dust	0.84 ~ 0.89	34 ~ 44	–
Barley	0.43 ~ 0.75	27 ~ 45	–

positions in the graph was found, and SF values of the horizontal and vertical coordinate axes were calculated in reverse.

According to the results shown in Table 4, the SF obtained by the two axis indexes is basically consistent within the allowable range of error, and the average SF value is used as the output value of the stability chart method. The results of this case are in line with the stability of the slope position corresponding to the actual site, which verifies that the graphic method based on the modified MC criterion proposed in this paper can make a preliminary SF estimation. In fact, the proposed modified MC technique is able to provide some guidance for the subsequent stability analysis.

6 Conclusions

A stability chart based on the modified MC criterion is presented for granular slopes in this study. The parameters of the new chart are basically the same as those included in the chart using the traditional MC criterion (ϕ , slope height, slope angle, natural density of materials and SF). The purpose of modifying the traditional MC criterion is to use only the accurate internal friction angle parameter obtained from the physical and mechanical experiments of granular materials, to eliminate the influence of the inaccurate cohesion parameter in the experiment for medium materials and to obtain another strength parameter of granular materials so that the stability analysis of granular slopes is closer to reality.

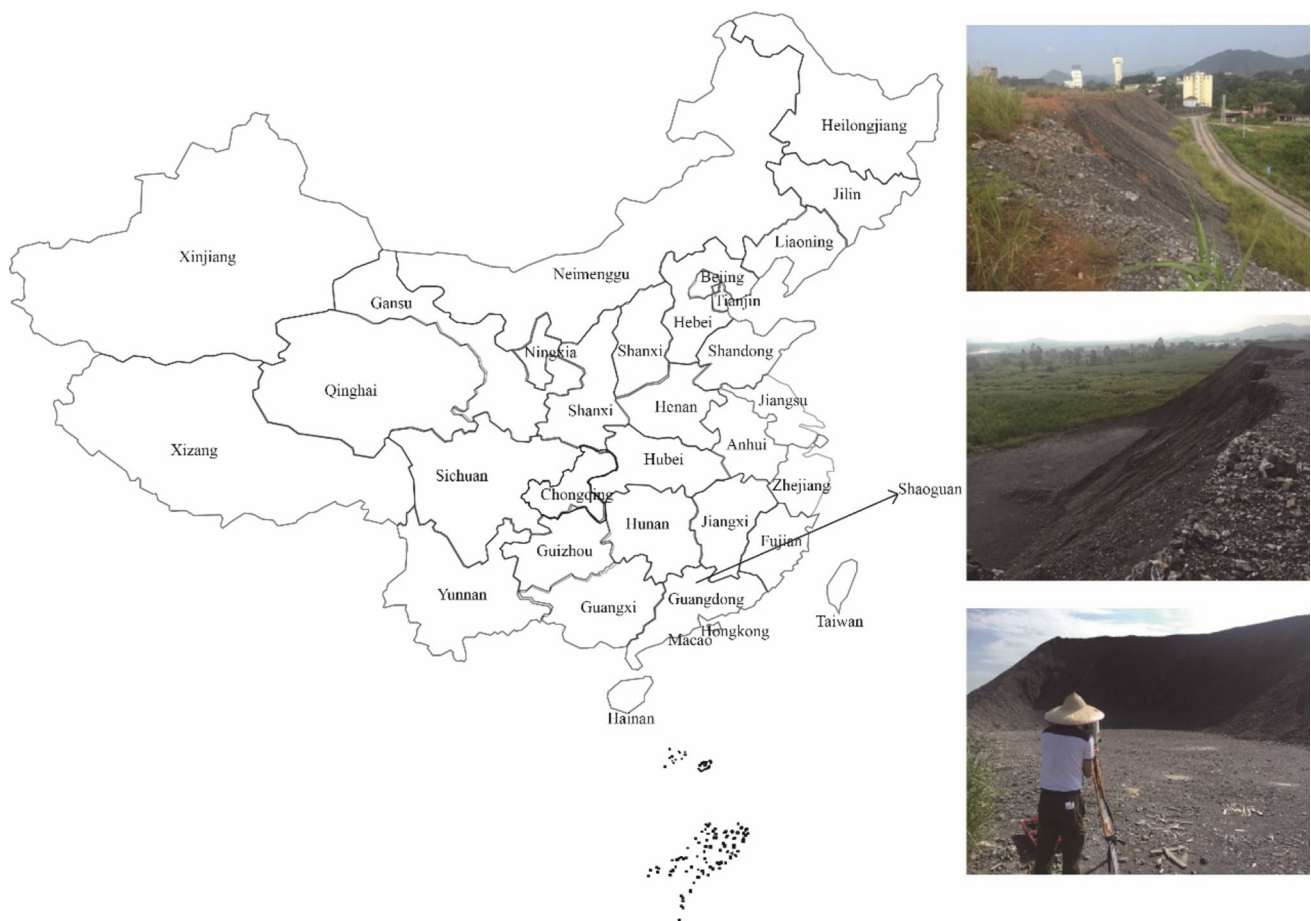


Fig. 17 Granular slope in the Fankou lead–zinc mine

First, physical and mechanical experiments were carried out on medium materials according to the experimental operation manual, and several data sets composed of c and ϕ were obtained, but only an average value of ϕ . The modified MC criterion parameter τ_0 was used to form the improved traditional MC criterion.

Second, in the modified MC criterion, the relationship between input parameters and output parameters becomes a simple one-to-one correspondence between ϕ and the shear strength, which rejects at the source the influence of the “un-real cohesion” obtained from the physical and mechanical experiments.

Third, according to the previous definition of medium materials and physical properties analysis, the range of ϕ for medium materials is basically defined as 15 ~ 55 degrees. The core of the stability chart proposed in this paper is the dimensionless stability number. Based on the modified MC criterion, when the shape of the slope and the DR are determined, the dimensionless stability number is only related to the ϕ of the granular materials, which is one of the special relations of the granular slope, which directly indicates that

the traditional strength parameter, cohesion, may not exist in the granular slope.

Fourth, based on the modified MC stability chart, this paper preliminarily determined the SF of the granular slope. When the geometric and strength parameters of the slope are determined, the unique coordinates can be determined in the stability chart, so the horizontal and vertical coordinate values containing the safety coefficient can be read. Finally, the two safety coefficient values can be calculated in reverse for comparison. The result is considered desirable if the error is within tolerance.

The research content and the proposed new viewpoints are intended to offer preliminary assessment on the stability analysis of granular slopes and provide guidance for the stability analysis and construction design of granular slope engineering. However, although the improved MC criterion has been verified in this paper, there are still different granular slopes with various strength properties that need to be considered to improve the criterion to increase its reliability and universality.

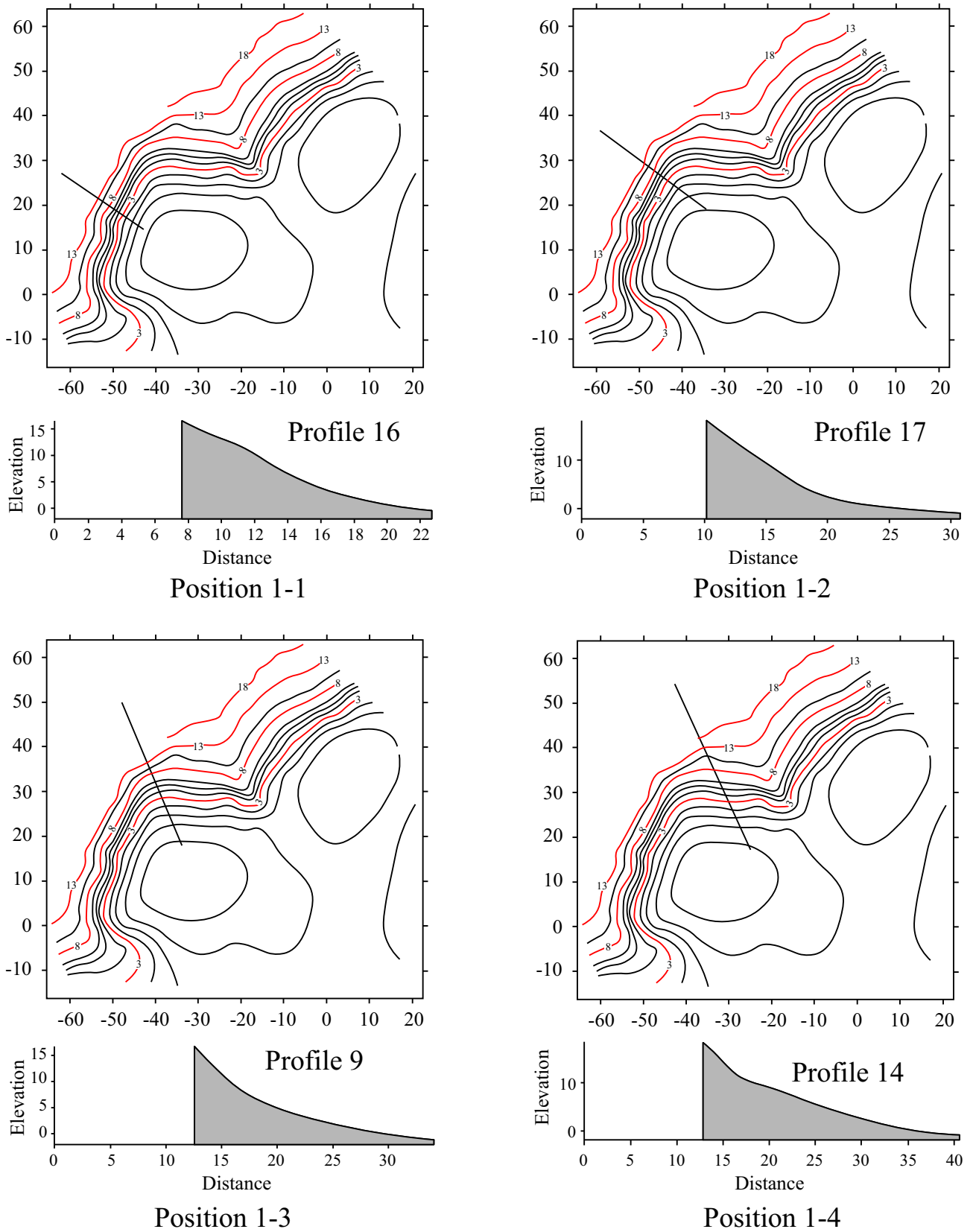


Fig. 18 Profile views of four specific positions on the granular slope



Fig. 19 Direct shear test of medium materials

Table 2 Direct shear test data

Position	Measured cohesion	Measured internal friction angle
1-1	165.99	49.9
1-2	152.41	49.3
1-3	99.30	44.0
1-4	59.18	40.9

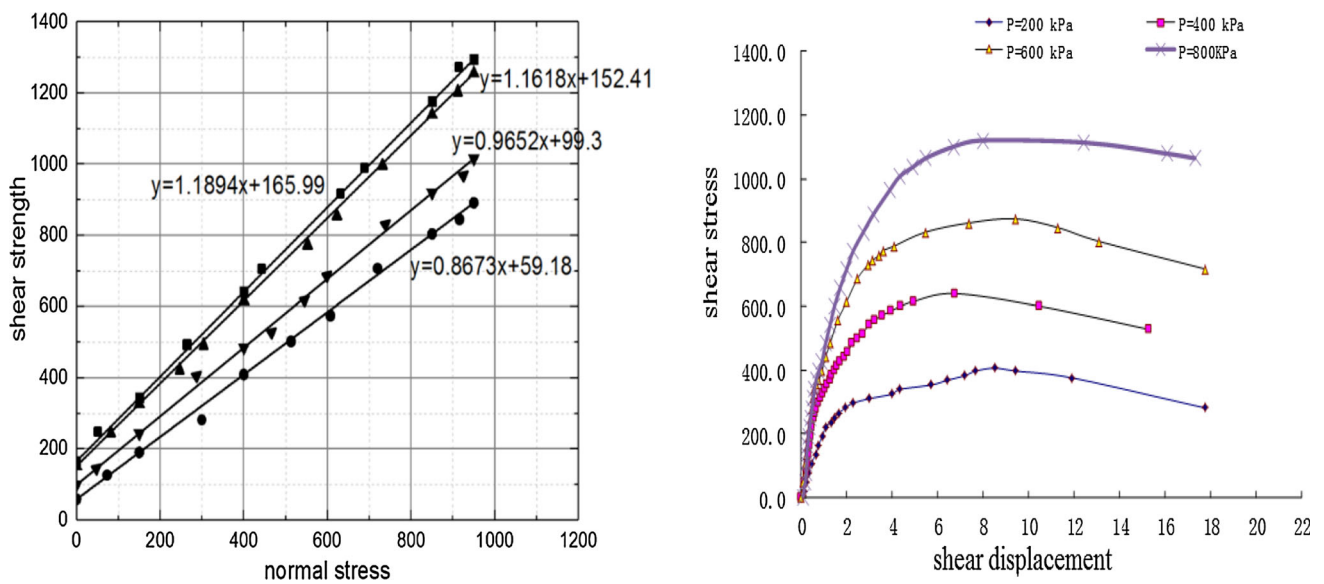


Fig. 20 Recording graphs of direct shear test data

Table 3 Modified MC criterion main parameters and slope geometry

Position	Angle of slope	Density	Initial shear stress	Inter friction angle
1–1	30	32.68	2.336	49.9
1–2	35	29.03	2.125	49.3
1–3	45	22.58	1.881	44.0
1–4	55	21.50	1.926	40.9

Table 4 Safety factor of the horizontal and vertical coordinate axis

Position	Horizontal safety factor	Vertical safety factor	Safety factor average
1–1	3.042	3.125	3.084
1–2	2.344	2.373	2.359
1–3	1.201	1.192	1.197
1–4	0.800	0.795	0.798

Acknowledgements This research is partially supported by the Distinguished Youth Science Foundation of Hunan Province of China (2022JJ10073) and the Innovation-Driven Project of Central South University (2020CX040).

Funding Open access funding provided by HEAL-Link Greece.

Declarations

Competing interests The authors declare that they have no known competing financial interests or personal relationships that could have appeared to influence the work reported in this paper.

Open Access This article is licensed under a Creative Commons Attribution 4.0 International License, which permits use, sharing, adaptation, distribution and reproduction in any medium or format, as long as you give appropriate credit to the original author(s) and the source, provide a link to the Creative Commons licence, and indicate if changes were made. The images or other third party material in this article are included in the article's Creative Commons licence, unless indicated otherwise in a credit line to the material. If material is not included in the article's Creative Commons licence and your intended use is not permitted by statutory regulation or exceeds the permitted use, you will need to obtain permission directly from the copyright holder. To view a copy of this licence, visit <http://creativecommons.org/licenses/by/4.0/>.

References

- Koronakis, N.; Kontothanassis, P.; Kazilis, N.; Gikas, N.: Stabilization measures for shallow tunnels with ongoing translational movements due to slope instability. *Tunn. Undergr. Space Technol.* **19**(4–5), 495 (2004)
- Brawner, C.O., Wyllie, D.: Rock slope stability on railway projects. *Area Bullet.* **77** (Bulletin 656) (1976)
- Liang, R.Y.; Nusier, B.O.; Malkawi, A.H.: A reliability based approach for evaluating the slope stability of embankment dams. *Eng. Geol.* **54**(3–4), 271–285 (1999)
- Psarropoulos, P.N.; Tsompanakis, Y.: Stability of tailings dams under static and seismic loading. *Can. Geotech. J.* **45**(5), 663–675 (2008)
- Zhou, J.; Qiu, Y.; Armaghani, D. J.; Zhang, W.; Li, C.; Zhu, S.; Tarinejad, R.: Predicting TBM penetration rate in hard rock condition: a comparative study among six XGB-based metaheuristic techniques. *Geosci. Front.* **12**(3), 101091 (2021)
- Zhou, J.; Huang, S.; Qiu, Y.: Optimization of random forest through the use of MVO, GWO and MFO in evaluating the stability of underground entry-type excavations. *Tunn. Undergr. Space Technol.* **124**, 104494 (2022)
- Li, C.; Zhou, J.; Armaghani, D. J.; Cao, W.; Yagiz, S.: Stochastic assessment of hard rock pillar stability based on the geological strength index system. *Geomech. Geophys. Geo-Energ. Geo-Resour.* **7**(2), 1–24 (2021)
- Iverson, R.M.; George, D.L.; Logan, M.: Debris flow runup on vertical barriers and adverse slopes. *J. Geophys. Res. Earth Surf.* **121**(12), 2333–2357 (2016)
- Chousianitis, K.; Del Gaudio, V.; Sabatakakis, N.; Kavoura, K.; Drakatos, G.; Bathrellos, G.D.; Skilodimou, H.D.: Assessment of earthquake-induced landslide hazard in Greece: from arias intensity to spatial distribution of slope resistance demand assessment of earthquake-induced landslide hazard in Greece. *Bull. Seismol. Soc. Am.* **106**(1), 174–188 (2016)
- Vishal, V.; Siddique, T.; Purohit, R.; Phophliya, M.K.; Pradhan, S.P.: Hazard assessment in rockfall-prone Himalayan slopes along national Highway-58, India: rating and simulation. *Nat. Hazards* **85**(1), 487–503 (2017)
- Wang, B.; Vardon, P.J.; Hicks, M.A.: Rainfall-induced slope collapse with coupled material point method. *Eng. Geol.* **239**, 1–12 (2018)
- De Vita, P.; Napolitano, E.; Godt, J.W.; Baum, R.L.: Deterministic estimation of hydrological thresholds for shallow landslide initiation and slope stability models: case study from the Somma-Vesuvius area of southern Italy. *Landslides* **10**(6), 713–728 (2013)
- Reale, C.; Xue, J.; Pan, Z.; Gavin, K.: Deterministic and probabilistic multi-modal analysis of slope stability. *Comput. Geotech.* **66**, 172–179 (2015)
- Gordan, B.; Armaghani, D.J.; Adnan, A.B.; Rashid, A.S.A.: A new model for determining slope stability based on seismic motion performance. *Soil Mech. Found. Eng.* **53**(5), 344–351 (2016)
- Kumar, J.; Samui, P.: Stability determination for layered soil slopes using the upper bound limit analysis. *Geotech. Geol. Eng.* **24**(6), 1803–1819 (2006)

16. Shen, H.; Klapperich, H.; Abbas, S.M.; Ibrahim, A.: Slope stability analysis based on the integration of GIS and numerical simulation. *Autom. Constr.* **26**, 46–53 (2012)
17. Fawaz, A.; Farah, E.; Hagechehade, F.: Slope stability analysis using numerical modelling. *Am. J. Civil Eng.* **2**(3), 60–67 (2014)
18. Mahdiyar, A.; Hasanipanah, M.; Armaghani, D.J.; Gordan, B.; Abdullah, A.; Arab, H.; Majid, M.Z.A.: A Monte Carlo technique in safety assessment of slope under seismic condition. *Eng. Comput.* **33**(4), 807–817 (2017)
19. Li, L.; Wang, Y.; Cao, Z.; Chu, X.: Risk de-aggregation and system reliability analysis of slope stability using representative slip surfaces. *Comput. Geotech.* **53**, 95–105 (2013)
20. Chiu, C.F.; Yan, W.M.; Yuen, K.V.: Reliability analysis of soil–water characteristics curve and its application to slope stability analysis. *Eng. Geol.* **135**, 83–91 (2012)
21. Samui, P.: Slope stability analysis: a support vector machine approach. *Environ. Geol.* **56**(2), 255–267 (2008)
22. Samui, P.: Utilization of relevance vector machine for rock slope stability analysis. *Int. J. Geotech. Eng.* **5**(3), 351–355 (2011)
23. Samui, P.; Lansivaara, T.; Kim, D.: Utilization relevance vector machine for slope reliability analysis. *Appl. Soft Comput.* **11**(5), 4036–4040 (2011)
24. Samui, P.: Support vector classifier analysis of slope. *Geomat. Nat. Haz. Risk* **4**(1), 1–12 (2013)
25. Samui, P.; Lansivaara, T.; Bhatt, M.R.: Least square support vector machine applied to slope reliability analysis. *Geotech. Geol. Eng.* **31**(4), 1329–1334 (2013)
26. Zhou, J.; Li, E.; Yang, S.; Wang, M.; Shi, X.; Yao, S.; Mitri, H.S.: Slope stability prediction for circular mode failure using gradient boosting machine approach based on an updated database of case histories. *Saf. Sci.* **118**, 505–518 (2019)
27. Gordan, B.; Armaghani, D.J.; Hajihassani, M.; Monjezi, M.: Prediction of seismic slope stability through combination of particle swarm optimization and neural network. *Eng. Comput.* **32**(1), 85–97 (2016)
28. Koopialipoor, M.; Armaghani, D.J.; Hedayat, A.; Marto, A.; Gordan, B.: Applying various hybrid intelligent systems to evaluate and predict slope stability under static and dynamic conditions. *Soft. Comput.* **23**(14), 5913–5929 (2019)
29. Singh P, Bardhan A, Han F, Samui P, Zhang W: A critical review of conventional and soft computing methods for slope stability analysis. *Model. Earth Syst. Environ.* 1–17 (2022)
30. Bardhan, A.; Samui, P.: Application of artificial intelligence techniques in slope stability analysis: a short review and future prospects. *Int. J. Geotech. Earthquake Eng. (IJGEE)* **13**(1), 1–22 (2022)
31. Bui, X. N.; Nguyen, H.; Choi, Y.; Nguyen-Thoi, T.; Zhou, J.; Dou, J.: Prediction of slope failure in open-pit mines using a novel hybrid artificial intelligence model based on decision tree and evolution algorithm. *Sci. Rep.* **10**(1), 1–17 (2020)
32. Asteris, P. G.; Mamou, A.; Ferentinou, M.; Tran, T. T.; Zhou, J.: Predicting clay compressibility using a novel Manta ray foraging optimization-based extreme learning machine model. *Transp. Geotech.* **37**, 100861 (2022)
33. Taylor, D.W.: Stability of earth slopes. *J. Boston Soc. Civ. Eng.* **24**(3), 197–246 (1937)
34. Michalowski, R.L.: Stability charts for uniform slopes. *Geotech. Geoenviron. Eng.* **128**(4), 351–355 (2002)
35. Klar A, Aharonov E, Kalderon-Asael B, Katz O: Analytical and observational relations between landslide volume and surface area. *J. Geophys. Res. Earth Surf.* **116**(F2) (2011)
36. Sun, J.; Zhao, Z.: Stability charts for homogenous soil slopes. *J. Geotech. Geoenviron. Eng.* **139**(12), 2212–2218 (2013)
37. Eid, H.T.: Stability charts for uniform slopes in soils with nonlinear failure envelopes. *Eng. Geol.* **168**, 38–45 (2014)
38. Vo, T.; Russell, A.R.: Stability charts for curvilinear slopes in unsaturated soils. *Soils Found.* **57**(4), 543–556 (2017)
39. Carranza-Torres C: Some comments on the application of the Hoek-Brown failure criterion for intact rock and rock masses to the solution of tunnel and slope problems. In: Barla M (eds) *MIR 2004-X Conference on Rock and Engineering Mechanics*. 24–25 Nov, Torino, Italy. Chap 10. Patron Editore. Bologna, pp 285–326
40. Li, A.J.; Merifield, R.S.; Lyamin, A.V.: Stability charts for rock slopes based on the Hoek-Brown failure criterion. *Int. J. Rock Mech. Min. Sci.* **45**(5), 689–700 (2008)
41. Li, A.J.; Merifield, R.S.; Lyamin, A.V.: Effect of rock mass disturbance on the stability of rock slopes using the Hoek-Brown failure criterion. *Comput. Geotech.* **38**(4), 546–558 (2011)
42. Li, A.J.; Lyamin, A.V.; Merifield, R.S.: Seismic rock slope stability charts based on limit analysis methods. *Comput. Geotech.* **36**(1–2), 135–148 (2009)
43. Shen, J.; Karakus, M.; Xu, C.: Chart-based slope stability assessment using the generalized Hoek-Brown criterion. *Int. J. Rock Mech. Min. Sci.* **64**, 210–219 (2013)
44. Sun, C.; Chai, J.; Xu, Z.; Qin, Y.; Chen, X.: Stability charts for rock mass slopes based on the Hoek-Brown strength reduction technique. *Eng. Geol.* **214**, 94–106 (2016)
45. Coulomb CA: *Essai sur une Application des regles de Maximis et Minimis a Quelques Problemes de Statique, Relatifs a l'architecture*. Volume 7 of, *Memoires de Mathematique & de Physique*, pp 343 (1976)
46. Mohr, O.: Welche Umstände bedingen die Elastizitätsgrenze und den Bruch eines materials? *Z. Ver. Dtsch. Ing.* **1900**(44), 1524–1530 (1900)
47. Wang Z: The rock coheres strength c and the rock angle of internal resistance nature. (in Chinese) *Proceedings of the 10th National Conference on Rock Mechanics and Engineering*, 226–231 (2008)
48. Bell, J.M.: Dimensionless parameters for homogeneous earth slopes. *J. Soil Mech. Found. Div.* **92**(5), 51–66 (1996)
49. Steward, T.; Sivakugan, N.; Shukla, S.K.; Das, B.M.: Taylor's slope stability charts revisited. *Int. J. Geomech.* **11**(4), 348–352 (2011)
50. Wood, A.M.M.: Tunnels for roads and motorways. *Q. J. Eng. Geol. Hydrogeol.* **5**(1–2), 111–126 (1972)
51. Hoek, E.; Carranza-Torres, C.; Corkum, B.: Hoek-Brown failure criterion. *Proc. NARMS Tac* **1**(1), 267–273 (2002)
52. Huang Songyuan (in Chinese) *Medium mechanics M.*: China Machine Press, (1993)
53. Клейн, Г.К. *Строительная механика сыпучих тел*. М.: Стройиздат, 256, 9 (1977)

